

Numerical reconstruction of digital holograms for three-dimensional shape measurement

Lihong Ma, Hui Wang, Yong Li and Hongzhen Jin

Information Optical Institute, Zhejiang Normal University, Jinhua 321004,
People's Republic of China

Received 8 January 2004, accepted for publication 19 February 2004

Published 12 March 2004

Online at stacks.iop.org/JOptA/6/396 (DOI: 10.1088/1464-4258/6/4/016)

Abstract

In this paper, we present a new technique for 3D shape measurement by recovering the 3D numerical reconstruction image of a digital hologram. Firstly, we fabricate a Fresnel digital hologram. Then, a number of 2D light field intensity distributions, which are in the reconstructed field of the digital hologram, are computed on the different depth planes. Finally, the focus measure evaluation of the grey level variance is applied. By finding the maximum focus measure, we decide on the depth information of each small image patch. The experiment confirms that the technique can materialize the 3D rebuilding of the reconstruction image and obtain 3D profile information on the object recorded. So digital holography can be a very promising technology for non-destructive 3D shape measurement.

Keywords: 3D shape measurement, digital holography, 3D reconstruction image, maximum focus measure

1. Introduction

Three-dimensional shape recovery of an object is an important topic in machine vision inspection and measurement tasks, which is widely used in many fields, such as industrial inspection, solid modelling, biomedicine, robot vision and so on. A variety of sensors and algorithms have been proposed [1–4], and generally they can be categorized into two types—active and passive—by the source used for sensing the objects of a scene. Both types of method have their own advantages and disadvantages. For example, active methods such as using laser beams need more complicated set-up and might be harmful to living objects, but their accuracy could be higher and more reliable. In contrast, passive methods such as shape from shading, shape from focus (image focus analysis, IFA), and stereo matching do not need extra equipment for active energy sources (which might be expensive in cost), and they are not limited by ambient light and the range of energy sources as active ones are, but the accuracy may not be as good as that of some active methods in some aspects. Many scientists deal with the topic of 3D shape recovery to achieve better algorithms and sensors.

Holography can record enough information for three-dimensional imaging. Conventional holography is usually

regarded as a realistic visualization of a 3D object. The recent development of a solid-state image sensor and a digital computer has enabled digital holography [5–10]. By digital holography, holograms are captured by a video camera and reconstructed by a computer by means of a diffraction integral. Theoretically, the holographic technique has a very high measuring sensitivity and accuracy. So digital holography is a very promising technique for 3D shape measurement. However, in previous studies digital holograms have been numerically reconstructed by means of changing the reconstruction distance, which is the distance between the hologram plane and the reconstruction plane. The alternative technique is that holograms have been numerically reconstructed by means of changing the viewing angles [8]. To some extent, both the techniques have not precisely obtained the 3D information, but rather only the 2D light field distribution. If we consider digital holography as a technique for 3D shape measurement, we must precisely extract the 3D information of a recorded object, that is, we must obtain the 3D reconstruction image.

In this paper, we will describe a new method to capture 3D information on an object by rebuilding the 3D numerical reconstruction image of a digital hologram. Firstly, a number

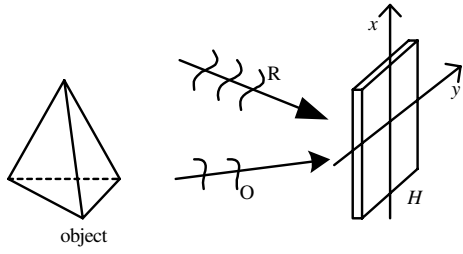


Figure 1. Optical sketch for recording Fresnel holograms: O, object wave; R, reference wave; H, hologram.

of 2D light field intensity distributions which are in the reconstructed field of the digital hologram are computed on the different depth planes. Then, the focus measure evaluation of the grey level variance is applied [11]. By finding the maximum focus measure, we decide on the depth information. The experiment confirms that the method can materialize the 3D rebuilding of the reconstruction image, that is, 3D profile information of the object can be obtained. So digital holography can be a practicable technology for non-destructive 3D shape measurement.

2. Numerical reconstruction of the digital hologram

The digital holography reported used a CCD target to directly record the hologram, which consisted of micro-interference patterns produced by the reference and object waves. Because of the limit of the low spatial resolution of a CCD, the size of the recorded object is limited. An in-line hologram can effectively use the pixels of a CCD, but the reconstructed image is limited by the presence of zero-order and conjugate images.

Here we adopt an approach to capture a digital hologram that is free from these limitations [12]. Firstly, as figure 1, we fabricate an off-axis Fresnel hologram recorded on a silver halide emulsion plate with enough resolution for interference fringes. Then, the fringes of the hologram are magnified by an optical imaging method. The geometry for optical magnification of the fringes is shown in figure 2. The illuminating wave must be a coherent wave. The distances μ and ν are related by the well known lens formula:

$$\frac{1}{\mu} + \frac{1}{\nu} = \frac{1}{f}. \quad (1)$$

The magnification multiple is

$$m = \frac{\nu}{\mu}. \quad (2)$$

By the Shannon sampling theorem, we do not put the hologram into a computer by scanning with high resolution until the frequency of the fringes is lower than half the resolution of the scanner. By this approach, the optical hologram is sampled into a digital hologram. In our laboratory, we scan the hologram using the ArtixScan 4000t slider scanner. With this we can obtain a maximal digital hologram approximately containing 5928×4132 pixels.

The numerical method used for hologram reconstruction simulates the standard optical reconstruction of a hologram. As we reconstruct a digital hologram, from the diffraction

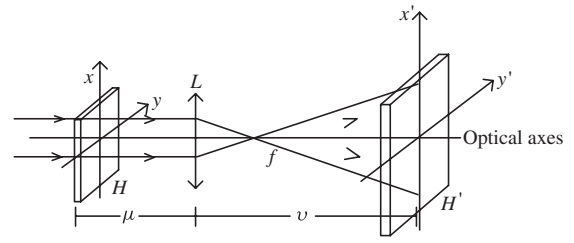


Figure 2. Optical sketch for magnifying the fringes of the hologram: L, lens; f , focal length; H, original recorded hologram; H', magnified hologram.

theory, a transmitted wavefront $U(x, y)$ is computed by multiplication of digital hologram $I(x, y)$ by a digitally computed illuminating wave $C(x, y)$. Taking into account the definition of the hologram intensity, we have

$$\begin{aligned} U(x, y) &= C(x, y)I(x, y) \\ &= C|R|^2 + C|O|^2 + CR^*O + CRO^*. \end{aligned} \quad (3)$$

The fourth term of the transmitted wavefront function $U(x, y)$ contains the exact conjugate object light wave, as the illuminating wave is the conjugation wave of the reference wave used when recorded, that is, $C(x, y) = R^*(x, y)$. So the real image can be reconstructed. In the propagation light field, 2D light field distributions can be computed at a number of planes parallel to the hologram. The 3D reconstruction image can be rebuilt and the photometric information can also be obtained by studying the light intensity distribution at the different planes. At a selected plane $P_{\xi\eta}$, which has a distance d from the hologram, the reconstructed conjugation object light wavefront $U_{id}(\xi, \eta)$, in the Fresnel approximation, is computed by the following equation:

$$\begin{aligned} U_{id}(\xi, \eta) &= A \iint O^*(x, y) \exp\left[i\frac{2\pi}{\lambda d}(x\xi + y\eta)\right] \\ &\quad \times \exp\left\{-\frac{i\pi}{\lambda d}(x^2 + y^2)\right\} \exp\left\{-\frac{i\pi}{\lambda d}(\xi^2 + \eta^2)\right\} dx dy. \end{aligned} \quad (4)$$

$O^*(x, y)$ can be expressed as the assembly of the spherical waves which converge at the different points (ζ_l, η_l, d_l) . The convergence points are the reconstructed image points. $|U_{id}(\xi, \eta)|^2$ is the 2D light field intensity distribution. In the selected plane, the integral result of function $U_{id}(\xi, \eta)$ is the δ function for the convergence points of $d_l = d$, that is, $|U_{id}(\xi, \eta)|^2$ obtains a maximum and the image points are obtained. But for those convergence points of d_l not equal to d , $|U_{id}(\xi, \eta)|^2$ becomes light speckle.

3. The algorithm for rebuilding the 3D reconstruction image

Reconstructing the hologram under certain conditions, the real image of the recorded object can be obtained. But using equation (4), we can only compute a 2D light field distribution at a plane which has a fixed distance from the hologram. The distribution is a mixed distribution of the focused image points and the defocused image speckles. As shown in figure 3, if the selected plane is associated with the image plane, a clear and focused image point is captured. However, if the selected plane does not coincide with the image plane and is displaced

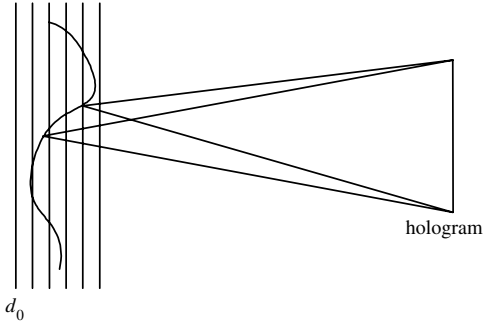


Figure 3. Sketch map of 2D reconstruction light field distributions at the different depth positions.

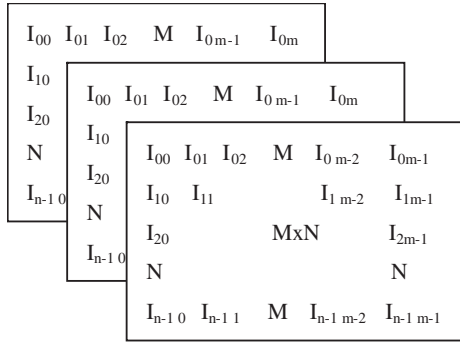


Figure 4. $M \times N$ matrix of the 2D reconstruction light field intensity distribution.

from it by a distance, the light intensity is distributed over a speckle on the selected plane. Thus for sufficiently contrasted and textured objects, when the selected plane associated with the image plane is found, the maximum grey level variance is obtained. Otherwise, the reconstruction image points will be blurred by different degrees depending on their distance from the image plane but also proportional to the distance. As a result, the grey level is averaged and the variance is small. All the 2D light field intensity distributions are processed by using the algorithm of the grey level variance evaluation to find the maximum grey level variance of each small patch of the reconstructed image. The relative depth information is then obtained.

As shown in figure 3, 2D light field intensity distributions are numerically reconstructed at different planes but the same interval in both the adjoining planes. Firstly, a series of 2D light field intensity distributions is computed. We study all the pixels in the plane of each 2D light field intensity distribution adopting matrix form. Assume that the number of acquired 2D light field intensity distributions is L and the computed pixels for each plane are $M \times N$. That is, $LM \times N$ matrices are acquired as in figure 4.

As mentioned above, the increase of both the adjoining reconstruction planes is constant, Δz . If the plane d_0 is regarded as the base plane, the relative depth of each 2D light field intensity distribution plane is computed by

$$z_k = d_0 - k\Delta z \quad k = 1, 2, \dots, L. \quad (5)$$

Let us consider the small surface patch which lies on the unknown surface of the reconstructed image and is

approximately normal to the hologram and approximately of the same depth. (This means that the object comprises many small patches, and the small patches must be much smaller than the distance from the object to the hologram.) Furthermore, the small patch is assumed to be a planar surface corresponding to a small region in the 2D light field distribution plane. Each plane consists of many such small regions. The small region is called the sample region. If each sample region has $m \times n$ pixels, the sequence of the sample regions is

$$m' = 1, 2, 3, \dots, M' \left(= \frac{M}{m} \right)$$

$$n' = 1, 2, 3, \dots, N' \left(= \frac{N}{n} \right).$$

On the selected reconstructing plane z_k , the focus measure of the (m', n') sample region is computed by

$$\gamma_{(m'n')z_k} = \frac{1}{m \times n} \sum_{i=1}^m \sum_{j=1}^n [I_{(m'n')z_k}(i, j) - \bar{I}_{(m'n')z_k}]^2. \quad (6)$$

In equation (6), $I_{(m'n')z_k}(i, j)$ is the intensity of each pixel in the (m', n') sample region on the plane z_k ; $\bar{I}_{(m'n')z_k}$ is the mean intensity value in the sample region. In the different computed planes, the (m', n') sample region corresponds. L values of the focus measure of the (m', n') sample region are acquired:

$$\gamma_{(m'n')z_1}; \gamma_{(m'n')z_2}; \gamma_{(m'n')z_3}; \dots; \gamma_{(m'n')z_L}. \quad (7)$$

The maximum focus measure is found by comparing the L values and the ordinal number K of the plane in which the maximum value exists is recorded. From equation (5), the relative depth of the small surface patch of the reconstructed image can be computed: $z_k = d_0 - k\Delta z$.

The procedure may be applied independently to all the sample regions in order to obtain the depth information of the entire reconstruction image. Besides, the coordinate x, y can be obtained by recording the ordinal number of the sample regions. As a result, the reconstructed image of the hologram can be rebuilt and the 3D information $(x_{m'}, y_{n'}, z_{m'n'})$ can be obtained.

4. Experimental result and conclusion

In this section we present and describe an experimental result using the above algorithm. As shown in figure 5(a), the model of a doll's head is the recorded object of the hologram. The maximum relative depth of the model is 1.5 cm. The size of the digital hologram is 5 mm \times 5 mm, containing 2500 \times 2500 pixels, and the nearest distance of the model from the hologram is 20 cm. By performing the integral of equation (4), 2D light field intensity distributions of the real image can be obtained. The acquired frame numbers are $L = 80$. Each plane contains 1998 \times 1998 pixels and the size of each pixel is 10 $\mu\text{m} \times 10 \mu\text{m}$. The increase of both the adjoining planes is 0.2 mm. When we compute the focus measure, the pixels of each sample region are 6 \times 6, and the number of the total sample regions is $M' = 333, N' = 333$. The interval of the acquired image points is 6 $\mu\text{m} \times 10 \mu\text{m}$. But in the interest of decreasing the data and clearly seeing the quality of the figure, we extract 66 \times 66 data from these data. Figure 5(b) presents the experimental result. In order to show

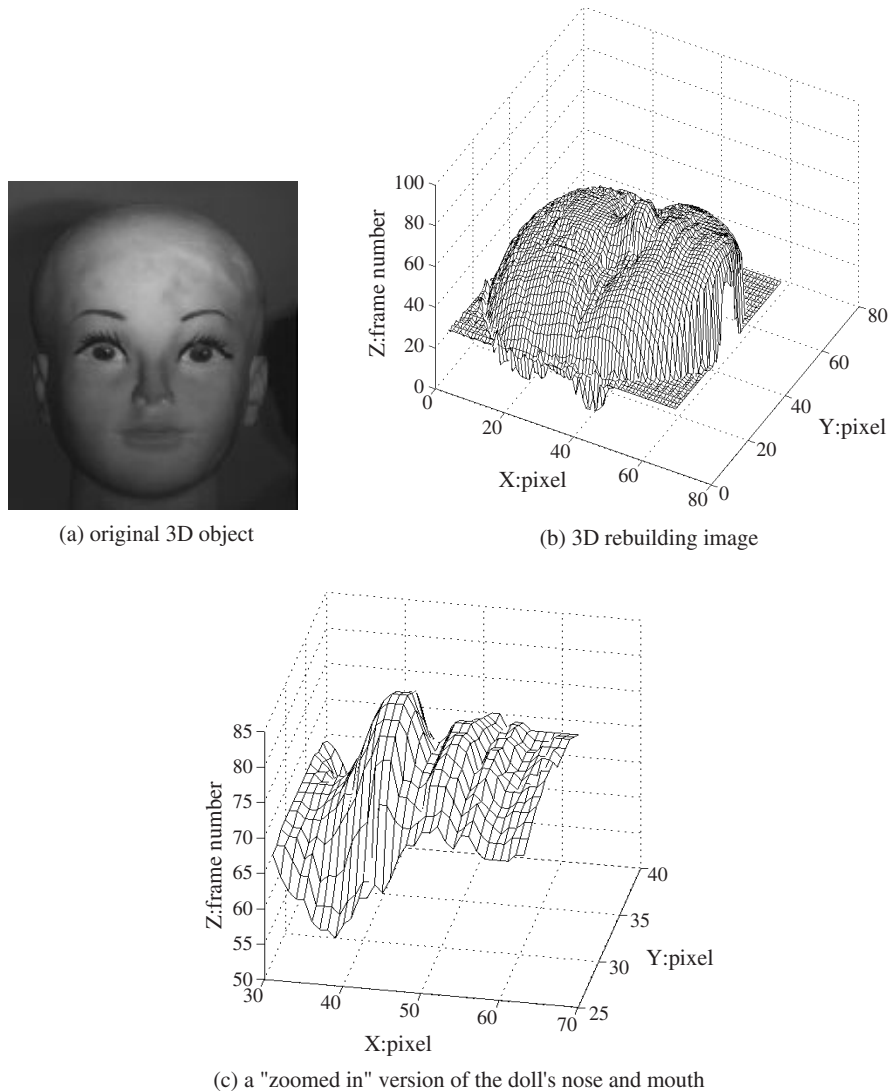


Figure 5. Experiment result.

the quality of the 3D information farther, we supply a 'zoomed in' version of the doll's nose and mouth as figure 5(c).

There are two trade-offs in the algorithm. First, frame numbers computed are considerably selected. Usually, we want to achieve the best shape recovery results that the displacement is as small as possible. But, if the displacement is smaller, the frame numbers are larger, and the computing cost is more consuming. The second trade-off is the sample region size versus the acquired image resolution. The smaller the size is, the higher the resolution is. However, the focus measure is more sensitive to noise and image overlap problems if the sample size is smaller, and it can result in the wrong depth estimate. The large window size is especially needed for those reconstructed images with low contrast regions. The optimal size can be acquired by trial experiments.

Experiments affirm that the method can materialize the 3D rebuilding of the reconstruction image and obtain 3D information on the object recorded. The method is a new technique for 3D object recovery. Theoretically, the holographic technique has a very high measuring sensitivity and accuracy. But the application of holographic technique

is much more complicated than other 3D shape measurements (especially the technique using white light e.g. projected fringe pattern and projected random pattern), not only in the hardware set-up and software algorithm, but also the requirement for the application environment. The measuring sensitivity and accuracy are affected by many factors during the course of recording the hologram, sampling the optical hologram into a digital hologram and applying the algorithm. So the problem of the measuring sensitivity and accuracy is very complicated and difficult. We are studying the problem and we will discuss it in other papers. In addition, this work will be continued in order to achieve better results and make the method a practicable method for 3D shape measurement.

References

- [1] Chen F, Brown G M and Song M 2000 Overview of three-dimensional shape measurement using optical methods *Opt. Eng.* **39** 10–2
- [2] Su X, Zou W, Von Bally G and Vukicevic D 1992 Automated phase measuring profilometry using defocused projection of a ronchi grating *Opt. Commun.* **94** 561–73

- [3] Su X, Von Bally G and Vukicevic D 1993 Phase-stepping grating profilometry: utilization of intensity modulation analysis in complex objects evaluation *Opt. Commun.* **98** 141–5
- [4] Yuan T and Subbarao M 1998 Integration of multiple-baseline color stereo vision with focus and defocus analysis for 3D shape measurement *Proc. SPIE Three-Dimensional Imaging Optical Metrology and Inspection IV; Proc. SPIE* **3520** 44–51
- [5] Schnars U, Kreis T M and Jüptner W P O 1996 Digital recording and numerical reconstruction of holograms: reduction of the spatial frequency spectrum *Opt. Eng.* **35** 977–82
- [6] Yamaguchi I and Zhang T 1997 Phase-shifting digital holography *Opt. Lett.* **22** 1268–70
- [7] Grilli S *et al* 2001 Whole optical wavefields reconstruction by digital holography *Opt. Express* **9** 294–302
- [8] Yu L, An Y and Cai L 2002 Numerical reconstruction of digital holograms with variable viewing angles *Opt. Express* **10** 1250–7
- [9] Naughton T J, Frauel Y, Javidi B and Tajahuerce E 2002 Compression of digital holograms for three-dimensional object reconstruction and recognition *Appl. Opt.* **20** 4124–32
- [10] Naughton T J, McDonald J B and Javidi B 2003 Efficient compression of Fresnel fields for internet transmission of three-dimensional images *Appl. Opt.* **23** 4758–64
- [11] Jarvis R A 1976 Focus optimization criteria for computer image processing *Microscope* **24** 163–80
- [12] Cai X 2001 Image reproduction of hologram by computer calculation *Appl. Laser* **21** 185–7